Mutational Effects on Conformational Changes of the Dephospho- and Phospho-forms of the Na^+,K^+-ATPase†

Mads Toustrup-Jensen, Majbritt Hauge, and Bente Vilsen*

Department of Physiology, University of Aarhus, Ole Worms Allé 160, DK-8000 Aarhus C, Denmark

Received October 11, 2000; Revised Manuscript Received February 26, 2001

ABSTRACT: Gly263 of the rat kidney Na^+,K^+-ATPase is highly conserved within the family of P-type ATPases. Mutants in which Gly263 or the juxtaposed Arg264 had been replaced by alanine were expressed at high levels in COS-1 cells and characterized functionally. Titrations of Na^+,K^+, ATP, and vanadate dependencies of Na^+,K^+-ATPase activity showed changes in the apparent affinities relative to wild-type compatible with a displacement of the E_1-E_2 conformational equilibrium in favor of E_1. The level of the K^+-occluded form was reduced in the Gly263→Ala and Arg264→Ala mutants, and the rate constant characterizing deocclusion of K^+ or Rb^+ was increased as much as 20-fold in the Gly263→Ala mutant. Studies of the sensitivity of the phosphoenzyme to K^+ and ADP showed a displacement of the E_1P-E_2P equilibrium of the phosphoenzyme in favor of E_1P, and dephosphorylation experiments carried out at 25 °C on a millisecond time scale using a quenched-flow technique demonstrated a reduction of the E_1P to E_2P conversion rate in the mutants. Hence, the mutations displaced the conformational equilibria of dephosphoenzyme and phosphoenzyme in parallel in favor of the E_1 and E_1P forms. The observed effects were more pronounced in the Gly263→Ala mutant compared with the Arg264→Ala mutant. Leu332 mutations that likewise displaced the conformational equilibria in favor of E_1 and E_1P were also studied. Unlike the Gly263→Ala mutant the Leu332 mutants displayed a wild-type like rate of K^+ deocclusion. Thus, the effect of the Gly263 mutation on the E_1-E_2 conformational equilibrium seems to be caused mainly by an acceleration of the K^+-deoccluding step, whereas in the Leu332 mutants the rate of the reverse reaction seems to be reduced.

The Na^+,K^+-ATPase[1] is a membrane bound enzyme found in the plasma membrane of all animal cells. It utilizes the free energy derived from the hydrolysis of ATP to transport Na^+ out of the cell and K^+ into the cell at a stoichiometry of 3:2, and is a member of the family of P-type ATPases characterized by the transfer during the functional cycle of the γ-phosphoryl of ATP to an aspartic acid residue located in the large cytoplasmic domain of the enzyme. The transport mechanism of the Na^+,K^+-ATPase is often described by the reaction sequence depicted in Scheme 1, the so-called "Albers-Post" or "E_1-E_2" model, which links ion movement to ATP hydrolysis through conformational changes mediating long-range interaction between the catalytic site and the cation transport sites in the membrane (*1*−*4*). The model considers at least two interconvertible phosphoenzyme conformations, E_1P and E_2P, and two dephosphoenzyme conformations, E_1 and E_2, and describes a consecutive mechanism of Na^+ and K^+ transport across the membrane.

Scheme 1: Minimum Reaction Cycle for the Na^+,K^+-ATPase[a]

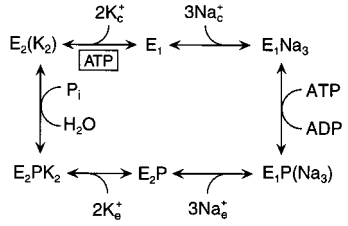

[a] The modulatory ATP binding to a low affinity site on E_2 is shown *boxed*. Occluded ions are shown in *parentheses*. *c* and *e* indicate cytoplasmic and extracellular sides, respectively.

The binding of three cytoplasmic sodium ions with high affinity to the enzyme in the E_1 form triggers the formation of a phosphoenzyme, E_1P, which is ADP sensitive, i.e., able to donate its phosphoryl group back to ADP forming ATP, and contains Na^+ in an occluded state (trapped within the protein). E_1P is spontaneously transformed into the "low energy" ADP-insensitive E_2P phosphoenzyme, and this transition is coupled with release of the sodium ions at the extracellular side of the membrane. The E_2P phosphoenzyme donates its phosphoryl group to water in a dephosphorylation reaction activated by the binding of extracellular K^+ with high affinity, leading to formation of an E_2 form with K^+ occluded. Binding of ATP at a low-affinity site on E_2 accelerates the transition to E_1. Thus, ATP has a dual role,

† This research was supported by grants from the Danish Medical Research Council, the NOVO Nordisk Foundation, and the Research Foundation of Aarhus University.

* To whom correspondence should be addressed. Fax: 45 86 12 90 65. E-mail: bv@fi.au.dk.

[1] Abbreviations: E_1 and E_2, conformational states of the Na^+,K^+-ATPase; EP, phosphorylated enzyme; $K_{0.5}$, ligand concentration giving half-maximum activation or inhibition; M1−M10, putative membrane segments numbered from the NH_2-terminal end of the peptide chain; Na^+,K^+-ATPase, the Na^+- and K^+-transporting adenosine triphosphatase (EC 3.6.1.37).

10.1021/bi002367m CCC: $20.00
Published on Web 04/12/2001

acting with high affinity it phosphorylates the enzyme, acting with low affinity and without phosphorylating, it facilitates the release of K^+ to the interior.

Although the E_1-E_2 and E_1P-E_2P conformational transitions have been studied extensively in the Na^+,K^+-ATPase isolated from kidney and salt glands by use of biochemical and biophysical techniques, such as proteolytic digestion, fluorescent probes, and ligand binding (*5*−*8*), the nature of these conformational changes remains obscure and it has not been determined whether the E_1P-E_2P conformational transition of the phosphoenzyme really resembles the E_1-E_2 transition of the dephosphoenzyme such as implied by the E_1/E_2 notation. Recently, analysis of the 3D crystal structure of the Ca^{2+}-ATPase in the E_1Ca_2 form and comparison with the 2D crystals obtained previously in the E_2-vanadate form has suggested a central role for the minor cytoplasmic domain connecting transmembrane segments M2 and M3 ("domain A" or "β-strand domain") in the E_1-E_2 conformational change (*9*). Proteolytic cleavage studies of the Na^+,K^+-ATPase have pointed to domain A as important for the coordination between structural changes of the phosphorylation site and the cation sites (*5*, *10*). A way to obtain more information on the conformational changes associated with ion transport is to use site-directed mutagenesis to pinpoint individual residues essential in this respect. Previously, the residue Leu332 located at the boundary between transmembrane segment M4 and the large cytoplasmic domain was shown by mutagenesis to play a pivotal role in the E_1P to E_2P conformational transition (*11*). Furthermore, Glu233 in domain A has been shown by mutagenesis to be important for the E_2 to E_1 transition of the dephosphoenzyme (*12*). In the present study, we have examined the possible involvement in the conformational changes of the residues Gly263[2] and Arg264 located close to the conformational sensitive proteolytic cleavage sites in the most COOH-terminal region of domain A. Both Gly263 and Arg264 were replaced by alanine. The conformational changes in the phosphoenzyme as well as the dephosphoenzyme were examined in studies of phosphorylation and dephosphorylation kinetics and by use of the inhibitor vanadate that reacts preferentially with the E_2 form during enzyme turnover. Quenched-flow measurements were for the first time applied on expressed mutant Na^+,K^+-ATPase to monitor on a millisecond time scale the transient kinetics of the phosphorylation reaction of Na^+,K^+-ATPase and the subsequent E_1P to E_2P transition. We have asked the question whether a displacement of the equilibrium between the E_1P and E_2P forms of the phosphoenzyme is linked with a displacement of the equilibrium between the E_1 and E_2 forms of the dephosphoenzyme, and the data demonstrate that the Gly263→Ala substitution causes substantial effects on the E_1-E_2 and the E_1P-E_2P equilibria. We have furthermore examined the conformational transition of the dephosphoenzyme in the mutants Leu332→Pro, and Leu332→Ala that like the Gly263→Ala mutant are characterized by accumulation of the E_1P form of the phosphoenzyme (*11*). Interestingly, the Gly263 and Leu332 mutants show widely differing behavior with respect to the kinetics of the conformational transition of the dephosphoenzyme.[3]

[2] All numbering of Na^+,K^+-ATPase residues in this article refers to the sequence of the rat α1 isoform. The residue in the sheep isoform equivalent to Gly263 of rat is Gly261.

MATERIALS AND METHODS

Mutagenesis, Transfection, and Selection. Base substitutions corresponding to the mutations Gly263→Ala and Arg264→Ala were introduced into cDNA encoding the ouabain-resistant rat α1 isoform of the Na^+,K^+-ATPase by use of oligonucleotide-directed mutagenesis (*13*, *14*). COS-1 cells were transfected with the wild-type and mutated rat α1 cDNA constructs, and ouabain-resistant colonies expressing exogenous rat Na^+,K^+-ATPases were selected by growth in the presence of 5 μM ouabain, expanded into stable cell lines, and up-regulated to the highest possible expression level by growth at extracellular K^+-concentrations lower than 1.5 mM, as before (*15*−*17*).

Plasma Membrane Isolation and Na^+,K^+-ATPase Activity Assays. Crude, NaI-treated plasma membranes were prepared from transfected COS-1 cells grown in medium containing ouabain (*15*), and protein concentration was determined using the dye binding method of Bradford (*18*). The plasma membranes were made leaky by use of sodium deoxycholate, and the Na^+,K^+-ATPase activity was measured as described previously (*15*, *16*) at 37 °C in the presence of 30 mM histidine (pH 7.4), 3 mM $MgCl_2$, 1 mM EGTA, 10 μM ouabain, and various concentrations of NaCl, KCl, and ATP. For assay of vanadate sensitivity, various concentrations of vanadate (ranging between 10^{-7} M and 5×10^{-4} M) were added from a stock solution of 1 M vanadate solubilized in excess NaOH. In all determinations of ATPase activity the reaction was initiated by adding 25 μL of leaky membrane solution containing 10 μg of total protein to 500 μL of assay medium, and the amount of P_i liberated over a period of 15 min was measured as previously described (*15*, *16*). To calculate the Na^+,K^+-ATPase activity referable to the expressed exogenous enzyme, the background ATPase activity measured with 10 mM ouabain added to inhibit all Na^+,K^+-ATPase activity was subtracted from the activity measured in the presence of 10 μM ouabain.

Studies of Phosphoenzyme at 0 °C and 10 °C. Studies of the Na^+ and K^+ dependencies of steady-state phosphorylation from ATP, the time course of ADP-dependent dephosphorylation, and the time course of dephosphorylation of phosphoenzyme formed at 600 mM NaCl to accumulate E_1P were carried out on the leaky membrane suspension (10 μg of total membrane protein preincubated with ouabain to inhibit the endogenous enzyme) at 0 °C as previously described in detail (*11*). For determination of the active site concentration, phosphorylation was carried out in the presence of 150 mM NaCl and oligomycin (20 μg/mL) to inhibit dephosphorylation (*11*). Deocclusion of K^+ or Rb^+ was studied in phosphorylation experiments at 10 °C (*19*, *20*). The background phosphorylation was determined in the presence of 50 mM KCl without NaCl.

Rapid Kinetic Phosphorylation and Dephosphorylation Studies. To perform rapid kinetic phosphorylation and dephosphorylation experiments at 25 °C, a Bio-Logic quench-flow module QFM-5 (Bio-Logic Science instruments, Claix, France) was used. This apparatus is designed to work with

[3] Part of this work was presented in preliminary form at the IXth International Conference on the Na/K-ATPase and related transport ATPases in Sapporo, Japan, August 1999, and at the 54th Annual Meeting and Symposium of the Society of General Physiologists, Woods Hole, MA, September 2000.

reaction volumes in the microliter range, as required in work with mutant pumps due to the tiny amount of protein available from the cell culture. The QFM-5 system can perform both single- and double-mixing experiments, using three or four reaction syringes, respectively, and can be operated in a continuous- or stopped flow mode. The apparatus is enclosed in a water jacket to allow temperature regulation of the reactant chambers and the reaction flow-line. All experiments described here were performed at 25 °C.

To monitor the phosphorylation rate of enzyme present in the Na^+-saturated form, single mixing experiments were performed ("Protocol 1"). Plasma membranes (0.1 mg/mL) suspended in 100 mM NaCl, 40 mM Tris (pH 7.4), 3 mM $MgCl_2$, 1 mM EGTA, 10 μM ouabain, and oligomycin (20 μg/mL) were mixed with an equal volume of the same buffer containing [γ-^{32}P]ATP (1, 2, 4, or 10 μM), followed by acid quenching at various time intervals by further mixing with an equal volume of 2.5 M phosphoric acid (titrated to pH 2.4 with NaOH). Reaction loop volumes (20 μL or 100 μL) and flow rate were varied to obtain reaction times between 11 and 300 ms.

To monitor the rate of the $E_1P \rightarrow E_2P$ transition, a double-mixing procedure was used to study dephosphorylation of phosphoenzyme formed in the presence of 600 mM NaCl to accumulate E_1P ("Protocol 2"). Plasma membranes (0.1 mg/mL) suspended in 600 mM NaCl, 40 mM Tris (pH 7.4), 3 mM $MgCl_2$, 1 mM EGTA, and 10 μM ouabain were mixed with an equal volume of the same buffer containing 4 μM [γ-^{32}P]ATP, and the flow was stopped for 5 s to obtain maximal phosphorylation. Dephosphorylation was initiated by mixing with the double volume of buffer of the same composition except for its content of NaCl, KCl, and unlabeled ATP, producing final concentrations of 20 mM KCl, 1 mM unlabeled ATP, and NaCl as described in the figure legend. Acid quenching was performed at various time intervals as described under Protocol 1. The aging time in the second reaction loop was varied between 10 ms and 110 ms by changing the flow rate.

The acid-precipitated ^{32}P-labeled phosphoenzyme was washed by centrifugation and subjected to SDS-polyacrylamide gel electrophoresis at pH 6.0 (*11, 20*), and the radioactivity associated with the separated Na^+,K^+-ATPase band was quantified by "imaging" using a Packard Cyclone Storage Phosphor System.

Background phosphorylation, obtained in similar but separate experiments in which 50 mM KCl replaced NaCl, was subtracted from each data point. The background phosphorylation was normally less than 5% for Protocol 1 experiments and less than 20% for Protocol 2 experiments, the difference being due to the length of the phosphorylation time (11−300 ms in Protocol 1 experiments and 5 s in Protocol 2 experiments).

Data Analysis and Statistics. Average values of several determinations of turnover rate are presented in Table 1. Each determination implies the measurement of the Na^+,K^+-ATPase activity at saturating concentrations of Na^+,K^+, and ATP, and the active site concentration by phosphorylation of the same deoxycholate activated membrane preparation on the same day and calculation of the ratio between these numbers. Because the Na^+,K^+-ATPase activity (expressed per milligram of total membrane protein) and the active site concentration determined by phosphorylation vary in parallel between various membrane preparations corresponding to the same mutant, the standard errors seen in Table 1 are relatively small.

Table 1: Apparent Affinities for ATP, Na^+, and K^+ and Turnover Rate for ATP Hydrolysis

mutant	$K_{0.5}$ (mM)[a]			turnover rate[b] (min^{-1})
	ATP	Na^+	K^+	
wild-type	0.435 ± 0.019 (n_H = 1.01)	9.85 ± 0.14 (n_H = 1.42)	0.615 ± 0.011 (n_H = 1.38)	8474 ± 165
Gly263→Ala	0.056 ± 0.003 (n_H = 0.94)	5.06 ± 0.14 (n_H = 1.69)	0.860 ± 0.033 (n_H = 1.37)	5017 ± 211
Arg264→Ala	0.276 ± 0.011 (n_H = 0.98)	8.01 ± 0.13 (n_H = 1.78)	0.587 ± 0.013 (n_H = 1.38)	9333 ± 369

[a] Determined by fitting the Hill equation to the complete set of normalized data points on which Figure 1 is based, as described under Materials and Methods. The Hill coefficient (n_H) and the SEM values obtained in the regression analysis are indicated as well. [b] The turnover rate was calculated as the ratio between the maximum Na^+,K^+-ATPase activity measured at 37 °C in the presence of 130 mM NaCl, 20 mM KCl, and 3 mM ATP, and the corresponding active site concentration determined on the same deoxycholate activated membrane preparation on the same day by phosphorylation at 0 °C in the presence of 150 mM NaCl together with oligomycin as described for Table 2 (see also ref *11*). Average values ± SEM of 9−12 such independent turnover determinations are shown.

Nonlinear regression analysis was carried out using the Sigmaplot program (SPSS, Inc.), and the best fits are shown as lines in the figures.

The Na^+,K^+, and ATP dependencies of the ATPase activity and the Na^+ dependency of the phosphorylation level were analyzed by applying the Hill equation:

$$V = (V_{max} - V_0)[L]^n/(K_{0.5}^n + [L]^n) + V_0$$

where V represents the ATPase activity or phosphorylation level, V_{max} its maximum value attained at infinite ligand concentration, and V_0 the value in the absence of the ligand. The data points shown in the graphs are average values corresponding to several independent determinations, often on various membrane preparations harvested over a period of more than a year. In each such determination, a titration corresponding to several ligand concentrations was performed. To calculate the average values shown in the graphs, each data point was first normalized relative to the V_{max} obtained by fitting the Hill equation to the data points obtained in the same titration. The $K_{0.5}$ values and Hill coefficients presented were subsequently calculated by refitting the Hill equation to the complete set of normalized data available from all the titrations.

The time dependence of phosphorylation of enzyme in the E_1 form was analyzed as a monoexponential time course. For determination of the K^+- or Rb^+-occluded enzyme and the rate constant corresponding to deocclusion, the time dependence of phosphorylation starting from a mixture of E_1 and the K^+- or Rb^+-occluded E_2 form was analyzed as a biphasic time course:

$$EP = (EP_{max} - E_{occluded})(1 - e^{-ht}) + E_{occluded}(1 - e^{-kt})$$

$E_{occluded}$ represents the part of the enzyme that phosphorylates slowly because of its initial presence as the occluded E_2 form. $EP_{max} - E_{occluded}$ is the fraction of the enzyme that phosphorylates almost instantaneously, because it is present as the nonoccluded form. Good fits to the data could be obtained

for all values of $h > 1\ s^{-1}$, without any significant variation of the values being determined for $E_{occluded}$ and the rate constant k corresponding to the slow phase. Consequently, the term $(1 - e^{-ht})$ was set equal to one for all the lines shown in Figures 8 and 9.

To predict the steady-state turnover rates for various choices of rate constants corresponding to the partial reactions in Scheme 1, a kinetic simulation software, SimZyme (*21*), was employed. SimZyme is based on the principles described in ref *22*. For any choice of reaction cycle and rate constants, the program solves the relevant differential equations, using the 4th order Runge−Kutta numerical method, and provides a graphical representation of the time dependence of the concentrations of the reaction intermediates and the rates of the individual partial reaction steps. A detailed description of a program with similar characteristics has previously been published (*23*). In the calculations referred to in the Discussion, it was assumed that under the prevailing conditions the pseudo-first-order rate coefficients for the binding of ions and ATP are more than 1 order of magnitude higher than the rate coefficients characterizing the major rate-limiting steps: $E_2 \rightarrow E_1$, $E_1 \rightarrow E_1P$, and $E_1P \rightarrow E_2P$. The reaction rates reported correspond to the steady-state situation reached after a reaction time of 10 s.

RESULTS

Expression and Ouabain Sensitivity. The amino acid substitutions Gly263→Ala and Arg264→Ala were introduced into the ouabain-resistant rat kidney Na^+,K^+-ATPase and the mutant enzymes were expressed in COS-1 cells as previously (*15*, *16*). Stable lines of COS-1 cells expressing mutant rat kidney Na^+,K^+-ATPase can be isolated following transfection and addition of ouabain to the growth medium, provided the mutant is functional, because the rat kidney enzyme is less sensitive to ouabain than the endogenous COS-1 cell Na^+,K^+-ATPase (*15*, *16*). Like the wild-type rat kidney Na^+,K^+-ATPase, both of the mutants conferred ouabain resistance to the COS-1 cells, indicating that the Gly263→Ala and Arg264→Ala substitutions are compatible with a Na^+,K^+-transport rate high enough to support cell growth. The mutant and wild-type Na^+,K^+-ATPases were expressed to active site concentrations in the range 25−60 pmol/mg of total membrane protein.

The ouabain concentration dependence of the ATPase activity was analyzed on plasma membranes isolated from the stable COS-1 cell lines expressing the mutants Gly263→Ala and Arg264→Ala or the wild-type Na^+,K^+-ATPase. Both of the mutants displayed a wild-type like affinity for ouabain, i.e., about 500-fold lower than that of the endogenous COS-1 cell Na^+,K^+-ATPase (results not shown). Thus, it can be excluded that the functional differences between the wild-type and the mutants Gly263→Ala and Arg264→Ala to be described below were caused by a change in ouabain sensitivity.

Na^+, K^+, and ATP Dependencies of Na^+,K^+-ATPase Activity. Figure 1 shows results of experiments in which the Na^+,K^+-ATPase activity was measured at various concentrations of Na^+,K^+, and ATP in expressed wild-type rat kidney Na^+,K^+-ATPase and the mutants Gly263→Ala and Arg264→Ala in the presence of 10 μM of ouabain to preferentially inhibit the ouabain-sensitive endogenous COS-1 cell Na^+,K^+-ATPase. Table 1 summarizes the ligand concentrations giving half-maximum activity ($K_{0.5}$) and also shows the maximum molecular activity (turnover rate) corresponding to the 100% values in Figure 1A. Compared with the wild-type, the Gly263→Ala mutant displayed a reduced $K_{0.5}$ for Na^+ (1.9-fold), a slightly increased $K_{0.5}$ for K^+ (1.4-fold), and a conspicuous 7.8-fold reduction in $K_{0.5}$ for ATP. In the wild-type Na^+,K^+-ATPase, the E_1 form binds Na^+ and ATP with high affinity, but K^+ with low affinity. The E_2 form, on the other hand, contains K^+ in an occluded state and binds ATP with low affinity (*4*). In connection with the K^+-deoccluding E_2 to E_1 conversion and the binding of Na^+ at the cytoplasmically facing sites of the E_1 form, the ATP site seems to undergo a structural change that allows ATP to bind with high affinity to the E_1Na_3 form and phosphorylate the enzyme. The E_2 to E_1 conversion is rate limiting for the overall reaction cycle and is accelerated by ATP binding at the low-affinity site on E_2, functioning as an allosteric modulatory site (boxed ATP in Scheme 1) (*3*, *24*). Due to

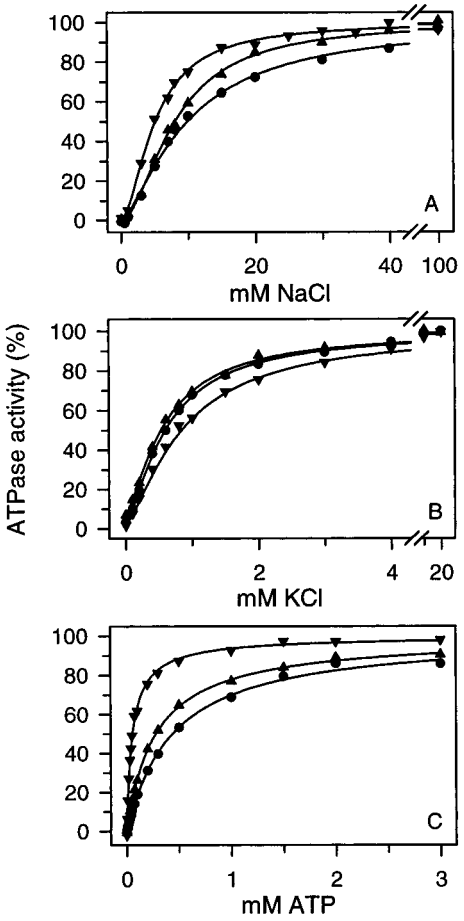

FIGURE 1: Na^+-, K^+-, and ATP dependencies of ATPase activity in the expressed wild-type Na^+,K^+-ATPase (●) and mutants Gly263→Ala (▼) and Arg264→Ala (▲). All measurements were carried out at 37 °C as described under Materials and Methods. At least five independent titrations were carried out corresponding to each line and the data points represent the average values calculated following normalization to the corresponding V_{max} as described under Materials and Methods. For all data points, SEM was less than 6%. The $K_{0.5}$ values and Hill numbers determined by fitting the Hill equation to the data are shown in Table 1. (A) Na^+ dependency, determined in the presence of 20 mM KCl and 3 mM ATP. (B) K^+ dependency, determined in the presence of 40 mM NaCl and 3 mM ATP. (C) ATP dependency, determined in the presence of 130 mM NaCl and 20 mM KCl.

Table 2: Characteristics of the Phosphoenzyme

mutant	$K_{0.5}(Na^+)$[a] (μM)	EP/(EP + oligomycin)[b] (%)	$K_{0.5}(K^+)$ (mM)	E_1P/E_2P (%)
wild-type	805 ± 25	74 ± 2	0.070[c]	33/67[d]
Gly263→Ala	655 ± 39	101 ± 1	40[c]	75/25[d]
Arg264→Ala	761 ± 30	79 ± 2	4.2[c]	70/30[d]
Leu332→Pro	466 ± 37[e]	102[e]	>60[e]	100/0[e]

[a] Phosphorylation was carried out for 15 s at 0 °C in the presence of 2 μM [γ-^{32}P]ATP, 3 mM $MgCl_2$, 1 mM EGTA, 10 μM ouabain, 20 mM Tris (pH 7.4), oligomycin (20 μg/mL), and various NaCl concentrations. The titrations were performed four to six times and each data point was normalized relative to the maximum phosphorylation obtained by fitting the Hill equation to the data points belonging to the same titration. The shown $K_{0.5}(Na^+)$ values ± SEM were then determined by refitting the Hill equation to the complete set of normalized data. The corresponding Hill numbers were 2.21, 2.41, and 2.22 for wild type, Gly263→Ala, and Arg264→Ala, respectively. [b] Phosphorylation was carried out as described above but in the presence of 150 mM NaCl without and with oligomycin (20 μg/mL). Each determination involved the measurement of phosphorylation with and without oligomycin on the same deoxycholate activated membrane preparation and the calculation of the ratio between these numbers. The average and the standard error were calculated from at least six such independent determinations of the ratio. [c] K^+ concentration giving half-maximum inhibition of phosphorylation, from Figure 2. [d] E_1P and E_2P from Figure 3. [e] Data from (*11*, *25*) included for comparison.

these characteristics of the enzyme, a mutation that displaces the E_1-E_2 equilibrium in favor of E_1 by accelerating the E_2 to E_1 conversion would be expected to result in a decrease in the $K_{0.5}$ value for ATP in titration of Na^+,K^+-ATPase activity (*3*, *4*, *12*, *19*, *24*) as well as some reduction in the $K_{0.5}$ value for Na^+. This corresponds to the behavior observed for the Gly263→Ala mutant. The Arg264→Ala mutant showed changes in affinities for ATP and Na^+ in the same direction as seen for the Gly263→Ala mutant, but the effects were less pronounced.

Na^+ Dependence of Phosphorylation. To determine the apparent Na^+ affinity also without K^+ present to compete with Na^+ at the ion-binding sites, the Na^+-dependence of phosphorylation from ATP was measured (Table 2). In these experiments oligomycin was present to inhibit dephosphorylation (see below). The $K_{0.5}$ for Na^+ displayed by the Gly263→Ala mutant was only 1.2-fold reduced relative to the wild-type and the $K_{0.5}$ for Na^+ was wild-type like in the Arg264→Ala mutant. Because the E_1 form prevails over the E_2 form in the absence of K^+, the intrinsic affinity of the E_1 form for Na^+ is more closely reflected by the $K_{0.5}$ for Na^+ determined in the phosphorylation assay, as compared with the $K_{0.5}$ value determined by the titration of ATPase activity depicted in Figure 1. The smaller magnitude of the mutational effect on the $K_{0.5}$ for Na^+ observed in the phosphorylation experiment, relative to that determined by titration of ATPase activity, is thus in accordance with the hypothesis that the mutations displace the E_1-E_2 equilibrium in favor of E_1, but leave the intrinsic Na^+ affinity of the E_1 form unaffected.

Oligomycin Effect on Phosphoenzyme Level and Maximum Molecular Activity (Turnover Rate). Table 2 furthermore shows the phosphorylation from ATP in the absence of oligomycin as percentage of the phosphorylation level reached in the presence of oligomycin. Because oligomycin stabilizes the Na^+-occluded form, thereby reducing the dephosphorylation rate, the phosphoenzyme level reached in the presence of oligomycin equals the active site concentration, whereas the steady-state phosphorylation level may be lower in the absence of oligomycin, depending on the rate of dephosphorylation. It is seen that in the wild-type the phosphorylation level reached in the absence of oligomycin was 74% that of the level reached in the presence of oligomycin. In the Arg264→Ala mutant, the corresponding value was 79%, whereas in the Gly263→Ala mutant the phosphorylation levels were identical in the presence and absence of oligomycin, indicating that the dephosphorylation rate is significantly reduced by the Gly263→Ala mutation, mimicking the effect of oligomycin.

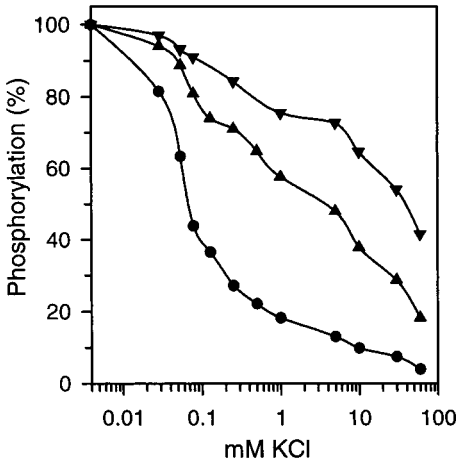

FIGURE 2: K^+ dependency of phosphorylation from ATP in the expressed wild-type Na^+,K^+-ATPase (●) and mutants Gly263→Ala (▼) and Arg264→Ala (▲). Phosphorylation was carried out for 15 s at 0 °C in the presence of 2 μM [γ-^{32}P]ATP, 20 mM NaCl, 20 mM Tris (pH 7.4), 3 mM $MgCl_2$, 1 mM EGTA, 10 μM ouabain, and various concentrations of KCl as indicated. The average values resulting from three to five independent determinations are shown as the percentage of the phosphoenzyme level obtained without KCl present. For all data points, SEM was less than 6%. The $K_{0.5}(K^+)$ values are shown in Table 2.

The molecular activity (turnover rate) was calculated from measurements of the maximum ATPase activity at saturating Na^+, K^+, and ATP concentrations and the active site concentration determined as the maximum capacity for phosphorylation in the presence of oligomycin (cf., refs *11* and *25*). As seen in Table 1, the turnover rate displayed by the Gly263→Ala mutant was significantly reduced (to 59%) compared with the wild-type, whereas the turnover rate of the Arg264→Ala mutant was wild-type like or tended to be slightly increased (to 110%) relative to that of the wild-type.

K^+ and ADP Sensitivities of the Phosphoenzyme. The phosphoenzyme is usually considered to consist of two major pools, E_1P and E_2P, which can be distinguished due to their different reactivities toward ADP and K^+. Thus, E_1P is K^+ insensitive but ADP sensitive, i.e., rapidly dephosphorylated by ADP due to its ability to donate the phosphoryl group back to ADP forming ATP, whereas E_2P is ADP insensitive and K^+ sensitive, i.e., rapidly hydrolyzed in the presence of K^+, binding at extracellularly facing sites. In the wild-type Na^+,K^+-ATPase, the major phosphoenzyme species accumulated at steady state in the presence of 20 mM Na^+ and absence of K^+ is the E_2P form, whereas at higher Na^+ concentrations, the E_1P-E_2P equilibrium is displaced toward E_1P.

To examine the K^+ sensitivity of the phosphoenzyme, phosphorylation was carried out at 0 °C in the presence of 20 mM Na^+ and varying K^+ concentrations. Figure 2 shows

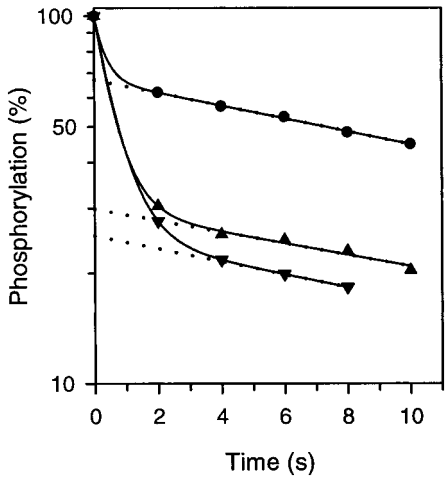

FIGURE 3: Time course of ADP-dependent dephosphorylation. The enzyme was phosphorylated for 10 s at 0 °C in the presence of 2 μM [γ-^{32}P]ATP, 20 mM NaCl, 20 mM Tris (pH 7.4), 3 mM $MgCl_2$, 1 mM EGTA, and 10 μM ouabain. Dephosphorylation was initiated by addition of a chase solution producing final concentrations of 2.5 mM ADP and 1 mM unlabeled ATP followed by acid quenching at the indicated time intervals. Average values of data points from 6 to 8 independent experiments were analyzed by fitting biexponential decay curves as previously described (*11*). For all data points, SEM was less than 3%. The rate coefficients corresponding to the slow and fast components, respectively, are the following: wild-type (●), 0.04 and 2.8 s^{-1}; Gly263→Ala (▼), 0.04 and 1.4 s^{-1}; Arg264→Ala (▲), 0.04 and 1.6 s^{-1}. The dotted lines show the extrapolation of the slow decay component corresponding to E_2P back to ordinate intercept. The extents of the two components are given in Table 2.

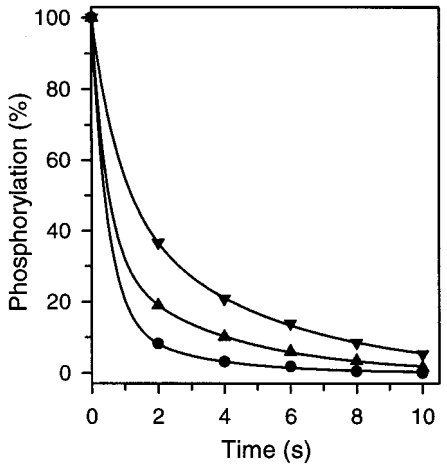

FIGURE 4: Dephosphorylation at 0 °C of phosphoenzyme formed at 600 mM NaCl. Phosphorylation was carried out for 10 s at 0 °C in the presence of 2 μM [γ-^{32}P]ATP, 600 mM NaCl (to accumulate the E_1P form), 20 mM Tris (pH 7.4), 3 mM $MgCl_2$, 1 mM EGTA, and 10 μM ouabain. Dephosphorylation was initiated by addition of a chase solution producing final concentrations of 100 mM NaCl, 20 mM KCl, and 1 mM unlabeled ATP, followed by acid quenching at the indicated time intervals. Average values of data points from six to eight independent experiments were analyzed by fitting biexponential decay curves as previously described (*11*). For all data points, SEM was less than 3%. The extent of the fast component and the rate coefficients corresponding to the fast and slow components, respectively, are the following: wild-type (●), 85%, 2.1 and 0.40 s^{-1}; Gly263→Ala (▼), 50%, 1.2 and 0.22 s^{-1}; Arg264→Ala (▲), 68%, 2.1 and 0.28 s^{-1}.

that in the wild-type the phosphoenzyme level was highly sensitive to micromolar concentrations of K^+ with half-maximum reduction being reached in the presence of approximately 70 μM K^+, in agreement with previous observations (*11*). On the other hand, both of the mutants Gly263→Ala and Arg264→Ala responded less strongly to K^+ with half-maximum reduction of the phosphoenzyme level being reached at K^+ concentrations approximately 600- and 60-fold higher, respectively, compared with wild-type (Figure 2 and Table 2). Furthermore, it is seen in Figure 2 that the decrease in the phosphoenzyme level induced by K^+ extends over a broader range of K^+ concentrations in the mutants than in the wild-type. The interpretation of the K^+ inhibition curves is complicated by the fact that at least two K^+ binding sites may be involved, but one important factor contributing to the K^+ insensitivity observed for the Gly263→Ala and Arg264→Ala mutants might be a change in the steady-state distribution of the phosphoenzyme intermediates, reducing the pool of K^+-sensitive E_2P.

By studying the time course of ADP-induced dephosphorylation of phosphoenzyme formed by phosphorylation from ATP in the presence of Na^+ and absence of K^+, an estimate of the E_1P-E_2P distribution can be obtained (*11*). Figure 3 and Table 2 show results of such kinetic experiments carried out following phosphorylation in the presence of 20 mM Na^+. It is seen in Figure 3 that the time course of ADP-induced dephosphorylation consisted of more than one exponential decay component. By fitting a biexponential function to the data points, the fractional amounts of E_1P and E_2P present initially were estimated from the extents of the rapid and slow decay components, respectively (Table 2). The dotted lines in Figure 3 show the extrapolation of the slow decay component back to ordinate intercept to indicate the amount of E_2P. In case of the wild-type, a high level of E_2P was accumulated at steady state, corresponding to an ordinate intercept of 67%, whereas in the Gly263→Ala and Arg264→Ala mutants, the amount of E_2P was reduced more than 2-fold, corresponding to ordinate intercepts of 25 and 30%, respectively. Hence, relative to the wild-type the distribution of E_1P and E_2P was changed in favor of E_1P in the mutants.

Dephosphorylation Kinetics of Phosphoenzyme Formed at 600 mM Na^+ (E_1P→E_2P Transition). To examine whether the accumulation of the E_1P phosphoenzyme in the mutants could be accounted for by a decrease in the rate of the E_1P→E_2P transition, experiments with the aim of comparing the rates of the E_1P→E_2P transition displayed by the wild-type and the mutants were carried out as described previously (*11*). First, the enzyme was phosphorylated from ATP in the presence of 600 mM Na^+. This high Na^+ concentration ensures accumulation of E_1P even in the wild-type (*11*, *26*). In accordance with this notion, the phosphoenzyme formed by the wild-type and the mutants under these conditions was found to be fully ADP-sensitive, i.e., it decayed within 2−4 s upon addition of ADP (data not shown). To observe the E_1P→E_2P transition, the dephosphorylation starting from E_1P was initiated by a downward jump in Na^+ concentration to 100 mM, and simultaneously 1 mM unlabeled ATP was added to terminate the phosphorylation reaction, together with 20 mM K^+ to ensure rapid dephosphorylation of E_2P. The dephosphorylation involves the steps E_1P→E_2P→E_2, but since the dephosphorylation step E_2P→E_2 is much faster than the E_1P→E_2P transition, the time course of phosphoenzyme decay reflects the rate of the latter reaction. Figure 4 shows that the dephosphorylation was significantly slower in the

mutants than in the wild-type, indicating that the $E_1P \rightarrow E_2P$ conversion rate is reduced in the mutants compared with the wild-type. The effect was more pronounced in the Gly263→Ala mutant than in the Arg264→Ala mutant. The decay curves consist of at least two components. Such heterogeneous kinetics of the E_1P decay has previously been observed for the wild-type Na^+,K^+-ATPase (*26*) and other mutants (*11*) and has been ascribed to heterogeneity of the lipid phase (*27*). The sum of two exponentials was fitted to the data, and the parameters extracted suggest a reduction of the extent of the rapid component and of the rate coefficient associated with the slow component in both of the mutants relative to the wild-type, more pronounced in the Gly263→Ala mutant than in the Arg264→Ala mutant. Moreover, in the Gly263→Ala mutant the rate coefficient associated with the rapid component was reduced almost to half that displayed by the wild-type Na^+,K^+-ATPase (for best fit parameters, see legend to Figure 4). It should be noticed that for the Arg264→Ala mutant it was also possible to obtain good fits in which the rate coefficient associated with the rapid component was reduced relative to wild-type, but then with less difference from the wild-type in the corresponding amplitude.

The phosphorylation and dephosphorylation experiments described above were carried out at 0 °C using a manual technique for addition of chase and quench solutions (*11*). To be able to correlate the mutational effects on the $E_1P \rightarrow E_2P$ transition with the turnover numbers for Na^+,K^+-ATPase activity, it was desirable to determine the decay of E_1P also at a more physiological temperature. By using the Bio-Logic quench-flow module QFM-5, it was possible to monitor the rate of the $E_1P \rightarrow E_2P$ transition on a millisecond time scale at 25 °C, even with the tiny amounts of expressed wild-type and mutant Na^+,K^+-ATPases available from the cell culture. The fast kinetic measurements of the $E_1P \rightarrow E_2P$ transition rate at 25 °C were in principle carried out in the same way as described above for 0 °C. The enzyme was phosphorylated for 5 s in the presence of 600 mM Na^+ followed by a downward jump in the Na^+ concentration (to 200 mM in this case) and acid quenching at various time intervals (Figure 5A). For comparison, we included in these experiments two additional mutants, Leu332→Pro and Leu332→Ala, for which it previously was shown that the E_1P form accumulates at 0 °C (*11*). The substituted residue Leu332 is thought to be located near the membrane surface in transmembrane segment M4, close to the cation-binding pocket (*9*, *16*, *19*, *28*).

As seen in Figure 5A, the dephosphorylation of the mutant Gly263→Ala was very much slowed relative to that of the wild-type Na^+,K^+-ATPase and coincided with that of the Leu332→Pro mutant, whereas in the mutants Arg264→Ala and Leu332→Ala the decay rate was intermediate between that of the wild-type and the former two mutants. Hence, the data indicate that also at 25 °C the $E_1P \rightarrow E_2P$ conversion rate was reduced in the mutants compared with the wild-type, and more so in the Gly263→Ala and Leu332→Pro mutants than in the Arg264→Ala and Leu332→Ala mutants. The decay curves consisted of at least two components such as those described above for 0 °C, and the sum of two exponentials was fitted to the data points (for parameters, see Table 3 and legend to Figure 5A). In the wild-type, the increase in temperature from 0 to 25 °C led to an increase in the rate coefficient associated with the rapid component from 2 to 112 s^{-1}, with the extent of the rapid component amounting to as much as 86% at 25 °C. Our data are in reasonable agreement with the rate constant of 60−77 s^{-1} determined at 20−21 °C and 100−120 mM Na^+ in dephosphorylation experiments on purified dog kidney and bovine brain Na^+,K^+-ATPase (*26*, *29*) and that of 98 s^{-1} determined in fluorescence experiments at 20 °C and 130 mM Na^+ on shark rectal enzyme (*30*). In the mutants, as well, the rapid phase constituted the major part of the decay at 25 °C, amounting to at least 70%, and the rate coefficient associated with the rapid phase was reduced as much as 4-fold in the Gly263→Ala and Leu332→Pro mutants, 2.6-fold in the Leu332→Ala mutant, and 2.0-fold in the Arg264→Ala mutant, relative to the wild-type.

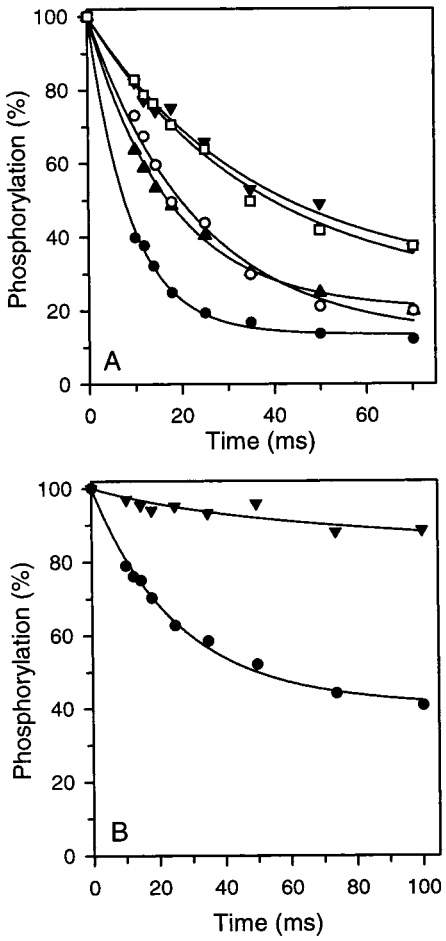

FIGURE 5: Rapid kinetic measurements at 25 °C of dephosphorylation of phosphoenzyme formed at 600 mM NaCl. The experiments were carried out using the QFM-5 module according to Protocol 2, see Materials and Methods. Dephosphorylation was initiated by addition of a chase solution producing final concentrations of 20 mM KCl, 1 mM unlabeled ATP, and (A) 200 mM NaCl or (B) 600 mM NaCl, followed by acid quenching at the indicated time intervals. Average values of data points from four to nine independent experiments were analyzed by fitting biexponential decay curves, and the best fits obtained using a fixed rate coefficient of 5×10^{-4} s^{-1} for the slow component are shown. For all data points, SEM was less than 6%. The extents of the fast components are the following. (A) wild-type (●), 86%; Gly263→Ala (▼), 71%; Arg264→Ala (▲), 79%; Leu332→Ala (○), 87%; Leu332→Pro (□), 75%. (B) wild-type (●), 57%; Gly263→Ala (▼), 8%. The rate coefficients corresponding to the fast components are given in Table 3 for panel A and are for panel B: wild-type (●), 40 s^{-1}; Gly263→Ala (▼), 28 s^{-1}. Note that there is considerable latitude in determination of the latter due to the low amplitude of only 8%.

Table 3: Mutational Effects on Reaction Rates, Deocclusion, and Vanadate Sensitivity

mutant	$E_1P \rightarrow E_2P$ rate[a] (s^{-1})	$E_2(K_2)$[b] (%)	$E_2(Rb_2)$[c] (%)	deocclusion rate[d] (s^{-1}) K^+	deocclusion rate[d] (s^{-1}) Rb^+	vanadate sensitivity[e] $K_{0.5}$ (μM)
wild-type	112	95	100	0.0096	0.0020	1.5
Gly263→Ala	28	46	93	0.1874	0.0420	10.7
Arg264→Ala	58	69	100	0.0408	0.0078	2.8
Leu332→Pro	28	46	78	0.0127	0.0076	39.4
Leu332→Ala	43	61	74	0.0147	0.0069	35.3

[a] Rate coefficient corresponding to the major part of the decay (fast component) in Figure 5A. [b] Relative amount of the K^+-occluded enzyme from Figure 8. [c] Relative amount of the Rb^+-occluded enzyme from Figure 9. [d] From Figures 8 and 9, rate coefficient corresponding to the slow component. [e] From Figure 10.

When similar experiments were conducted without any downward jump in salt concentration, i.e., by addition of a dilution medium containing 600 mM Na^+ and 20 mM K^+, both the extent and the rate coefficient associated with the rapid component was reduced in the wild-type (Figure 5B), as compared to the situation in which 200 mM Na^+ was present during dephosphorylation. Such a behavior is in agreement with previous studies and can be ascribed to a salt effect on the lipid phase, indirectly affecting the kinetic properties of the E_1P form and slowing conversion to E_2P (*26*, *27*). The salt also slowed the phosphoenzyme decay in the Gly263→Ala mutant and the difference between the decay curves of the wild-type and the Gly263→Ala mutant remained conspicuous at the high salt concentration. In fact, as seen from Figure 5B, the dephosphorylation of the Gly263→Ala mutant was extremely slow, with 90% of the phosphoenzyme remaining following dephosphorylation for 100 ms.

Phosphorylation of the E_1Na_3 Form. To elucidate whether the mutations Gly263→Ala, Arg264→Ala, Leu332→Pro, and Leu332→Ala interfered with the phosphorylation reaction itself [$E_1Na_3 \rightarrow E_1P(Na_3)$ in Scheme 1], the rate of phosphorylation by ATP was studied at 25 °C on enzyme preincubated in the presence of 100 mM Na^+ to saturate the Na^+ transport sites and oligomycin to block dephosphorylation, using the quench-flow module. Figure 6 shows the time course of phosphorylation of the expressed wild-type enzyme in the presence of 2 μM ATP. A monoexponential function could be satisfactorily fitted to the data as demonstrated by the line. Similar experiments were also conducted at ATP concentrations of 0.5, 1, and 5 μM, and a double reciprocal plot of the initial phosphorylation rate as a function of the ATP concentration is shown in the inset to Figure 6. The initial phosphorylation rate is in units of $(seconds)^{-1}$, because it is calculated relative to the enzyme concentration to obtain the rate per ATPase molecule. As seen, a straight line could be fitted to the data and the extrapolated maximum rate of phosphorylation corresponding to infinite ATP concentration is 138 s^{-1} and the K_m value 7 μM, in reasonable accordance with the respective values of 190 s^{-1} and 7 μM obtained on purified pig kidney Na^+,K^+-ATPase at 24 °C (*8*). To test the phosphorylation reaction in the mutants Gly263→Ala, Arg264→Ala, Leu332→Ala, and Leu332→Pro, the time course of phosphorylation was studied at 2 μM ATP, i.e., a concentration that is nonsaturating in the wild-type so that a change either in the maximum phosphorylation rate or in the K_m should be revealed. As shown by the lines in Figure 7, a monoexponential function could be fitted to the time dependence of phosphorylation following addition of ATP to the Na^+-saturated enzyme for each mutant, and the rate

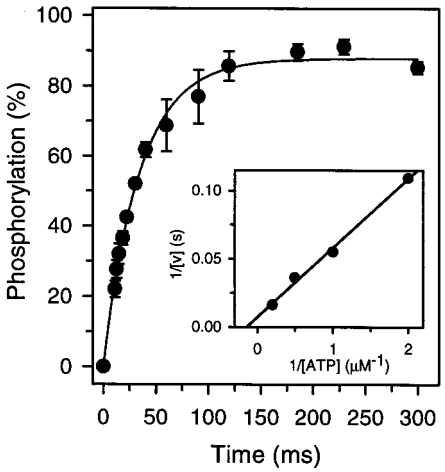

FIGURE 6: Rapid kinetic measurements at 25 °C of the time course of phosphorylation and (inset) ATP dependence of the initial rate of phosphorylation in the expressed wild-type Na^+,K^+-ATPase. The experiments were carried out using the QFM-5 module according to Protocol 1, see Materials and Methods, in the presence of 2 μM [γ-^{32}P]ATP or (inset) 0.5, 1, 2, or 5 μM [γ-^{32}P]ATP. Average values of data points from two to six independent experiments were analyzed by fitting a monoexponential time function. SEM values are indicated by the error bars. The 100% value corresponds to the active site concentration determined in phosphorylation experiments at 0 °C in the presence of 150 mM NaCl and oligomycin as described for Tables 1 and 2 (see also ref *11*). The rate coefficient is 29 s^{-1} and the maximum phosphorylation level 87.8%. The inset shows a double reciprocal plot of the initial rate (expressed relative to the enzyme concentration to obtain the molecular rate in s^{-1}) as a function of ATP concentration. The maximum rate for the phosphorylation reaction corresponding to infinite ATP concentration and the K_m value for ATP determined from this plot are 138 s^{-1} and 7 μM, respectively.

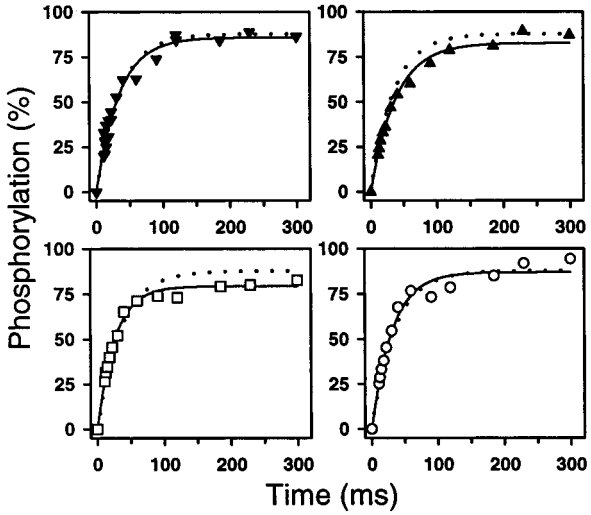

FIGURE 7: Rapid kinetic measurements at 25 °C of the time course of phosphorylation in mutants. The experiments were carried out at 2 μM [γ-^{32}P]ATP as described for Figure 6. Average values of data points from two independent experiments were analyzed by fitting a monoexponential time function. For all data points, SEM was less than 7%. The rate coefficients and the maximum phosphorylation level as percentage of the active site concentration determined as described for Figure 6 are the following: Gly263→Ala (▼), 29 s^{-1}, 85.9%; Arg264→Ala (▲), 26 s^{-1}, 82.8%; Leu332→Pro (□), 38 s^{-1}, 80.3%; Leu332→Ala (○), 32 s^{-1}, 87.1%. The dotted line shows the wild-type curve from Figure 6.

coefficients and maximum phosphorylation levels were generally very similar to those of the wild-type enzyme, a slight increase in the rate coefficient and a slight decease in the maximum phosphorylation level being noted for the Leu332→Pro mutant. Hence, the mutations do not appear to exert large effects that substantially reduce either the maximum phosphorylation rate or the affinity for ATP at the phosphorylation site of the E_1 form.

Deocclusion of K^+ and Rb^+. To study the time course of the $E_2(K_2)$→E_1 transition of the dephosphoenzyme at low ATP concentration, the previously described method (*19*) was applied. In short, the enzyme is incubated with K^+ in the absence of Na^+ and ATP to form the K^+-occluded intermediate, $E_2(K_2)$. Following equilibration with K^+, oligomycin is added and the enzyme is then phosphorylated by addition of [γ-^{32}P]ATP together with 100 mM Na^+. The time course of phosphorylation is biphasic, a rapid phase reflecting phosphorylation of the enzyme pool present initially as the nonoccluded E_1 form, followed by a slow phase reflecting deocclusion of the $E_2(K_2)$ enzyme pool with phosphorylation proceeding through the steps $E_2(K_2)$→E_1→E_1Na_3→$E_1P(Na_3)$ where the release of occluded K^+ is rate limiting. As phosphorylation of the E_1 enzyme pool, corresponding to the fast phase, is completed within 5 s, the phosphorylation data in Figures 8 and 9 were analyzed as a biphasic time function in which the component corresponding to the rapid phase is constant [cf., ref *19* and Materials and Methods]. The slow phase then reflects the K^+ deocclusion and its rate constant and amplitude [the relative amount of enzyme initially present in the $E_2(K_2)$ form] can be extracted from the best fit (lines shown in Figures 8 and 9).

Figure 8 and Table 3 depict the results of such experiments in which the mutants Gly263→Ala, Arg264→Ala, Leu332→Pro, and Leu332→Ala and the wild-type enzyme were preequilibrated with 8 mM K^+ at pH 7.5. Under these conditions, the wild-type Na^+,K^+-ATPase displayed almost no rapid phase of phosphorylation, indicating a close to 100% saturation of the K^+-occlusion sites, whereas the relative amount of the K^+-occluded form was reduced to less than 50% in the mutants Gly263→Ala and Leu332→Pro (see Table 3). In the wild-type enzyme, 100 μM K^+ is sufficient to saturate the K^+-occlusion sites 50% (see ◆ in Figure 8, taken from ref *20*), and, hence, the K^+ concentration required to saturate the K^+-occlusion sites 50% in the mutants Gly263→Ala and Leu332→Pro was at least 80-fold higher than that required in the wild-type enzyme. For Arg264→Ala and Leu332→Ala, the amount of K^+-occluded enzyme was reduced less, but the difference from the wild-type was substantial for these mutants as well (Table 3).

As further seen in Figure 8 and Table 3, the rate constant characterizing the deocclusion of K^+ was strongly increased in the Gly263→Ala mutant (20-fold) and moderately increased (4-fold) in the Arg264→Ala mutant, relative to the wild-type. By contrast, the corresponding rate constants displayed by the Leu332→Pro and Leu332→Ala mutants were not significantly increased relative to wild-type. The difference between the deocclusion rates of the Gly263→Ala mutant and the Leu332→Pro mutant is particularly noteworthy inasmuch as these mutants displayed about the same apparent affinity for K^+ (46% saturation at 8 mM K^+, cf. Table 3).

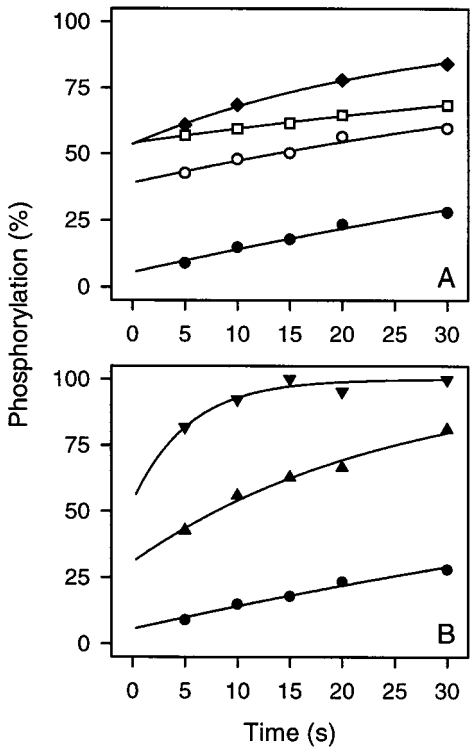

FIGURE 8: Time course of K^+ deocclusion in the wild-type Na^+,K^+-ATPase (●, ◆) and the mutants Gly263→Ala (▼), Arg264→Ala (▲), Leu332→Ala (○), and Leu332→Pro (□). Following preequilibration for 1 h at 25 °C, pH 7.5, with 8 mM KCl (●, ▼, ▲, ○, □), oligomycin was added and the enzyme was cooled to 10 °C and diluted 10-fold in a medium containing 1 μM [γ-^{32}P]ATP and 100 mM NaCl at 10 °C, and the phosphorylation was monitored as previously described (*19*, *20*). For determination of the 100% value (representing fully deoccluded enzyme corresponding to infinite time), the 1h incubation was carried out in the presence of 50 mM Na^+ and absence of K^+. Average values of data points from 3 to 11 independent experiments were analyzed by fitting a biphasic time function with one of the exponential terms being replaced by a constant due to the high rate coefficient (see Materials and Methods). For all data points, SEM was less than 7%. The extracted rate constant corresponding to the slow phase (deocclusion rate) and the extent of the slow phase, corresponding to the amount of $E_2(K_2)$, are shown in Table 3. Data obtained previously (*20*) for the wild-type Na^+,K^+-ATPase preequilibrated with 100 μM KCl (◆) are included for comparison.

To examine this difference between the deocclusion rates in more detail, experiments were carried out also under conditions where a larger fraction of the enzyme was initially present in the occluded state (Figure 9). This was achieved by replacing K^+ with Rb^+ and decreasing the pH to 6.5, conditions known to stabilize the occluded form of the wild-type Na^+,K^+-ATPase (*31*). Under these conditions, the extent of the slow phase increased to 100% in the wild-type and mutant Arg264→Ala, to 93% in mutant Gly263→Ala, and to 70−80% in the Leu332 mutants (Figure 9 and Table 3). In the wild-type as well as in the Gly263→Ala mutant, the rate of deocclusion of Rb^+ at pH 6.5 was about 5-fold lower than the rate of deocclusion of K^+ at pH 7.5. Thus, the 20-fold difference between the Gly263→Ala mutant and the wild-type was retained. For Leu332→Pro and Leu332→Ala, the rate of deocclusion of Rb^+ was only 3−4-fold higher than in the wild-type, thus confirming that in these mutants deocclusion occurs considerably slower than in mutant Gly263→Ala, even though the latter mutant displayed a

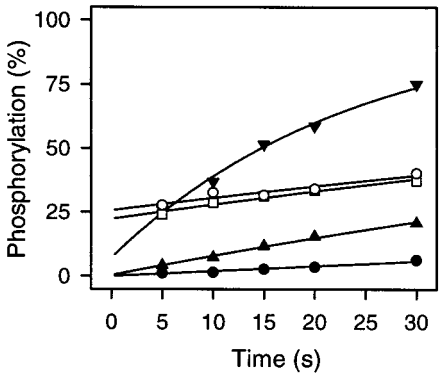

FIGURE 9: Time course of Rb^+ deocclusion in the wild-type Na^+,K^+-ATPase (●) and the mutants Gly263→Ala (▼), Arg264→Ala (▲), Leu332→Ala (○), and Leu332→Pro (□). The experiments were carried out as described for Figure 8, but at pH 6.5 following preequilibration with 8 mM RbCl at pH 6.5. Average values of data points from three to six independent experiments were analyzed as described for Figure 8. For all data points, SEM was less than 5%. The extracted rate constant corresponding to the slow phase (deocclusion rate) and the extent of the slow phase, corresponding to the amount of $E_2(Rb_2)$, are shown in Table 3.

higher apparent affinity for Rb^+ than the Leu332 mutants (Figure 9 and Table 3).

These data suggest that in the Gly263 mutant, the effect of the mutation on the E_1-E_2 conformational equilibrium is caused predominantly by an acceleration of the K^+-deoccluding E_2 to E_1 transition, whereas in the Leu332 mutants a reduced rate of the reverse E_1 to E_2 transition contributes considerably to the displacement of the conformational equilibrium in favor of E_1.

Vanadate Sensitivity. Vanadate inhibits the Na^+,K^+-ATPase by binding in competition with P_i forming a stable complex with the enzyme (*32*). As vanadate binds exclusively to the E_2 form, vanadate can be used as a conformational probe to obtain information about the E_1-E_2 conformational equilibrium of the dephosphoenzyme. Hence, a displacement of the conformational equilibrium in favor of E_1 would be expected to result in a reduced sensitivity to vanadate. Figure 10 shows the effects of varying concentrations of vanadate on the Na^+,K^+-ATPase activity in the wild-type and the mutants Gly263→Ala, Arg264→Ala, Leu332→Pro, and Leu332→Ala. The Hill-equation was fitted to the data points and the $K_{0.5}$ values for inhibition of the Na^+,K^+-ATPase activity by vanadate are shown in Table 3. Compared with the wild-type, the vanadate sensitivity and, thus, the amount of the vanadate-reactive E_2 form present at steady state, was reduced 1.9-, 7.0-, 24-, and 26-fold in the mutants Arg264→Ala, Gly263→Ala, Leu332→Ala, and Leu332→Pro, respectively.

DISCUSSION

In this study, mutants in which either Gly263 or the juxtaposed residue Arg264 of the rat kidney Na^+,K^+-ATPase had been replaced by alanine were functionally characterized, and mutational effects on the conformational equilibria of the phosphoenzyme as well as the dephosphoenzyme were revealed. Gly263 is highly conserved within the family of P-type ATPases, and in the crystal structure of the sarcoplasmic reticulum Ca^{2+}-ATPase, the glycine corresponding to Gly263 of the Na^+,K^+-ATPase is located at the boundary between a helix and a hydrogen-bonded turn that connects

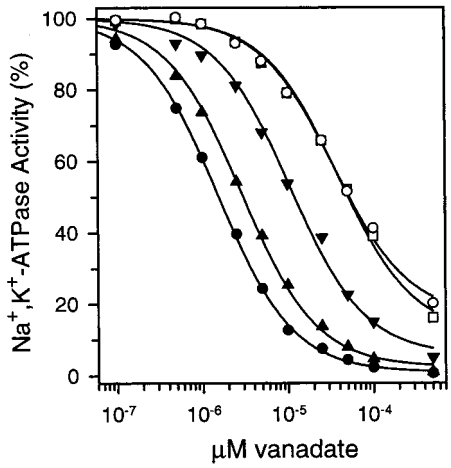

FIGURE 10: Vanadate-dependency of Na^+,K^+-ATPase activity of the wild-type Na^+,K^+-ATPase (●) and the mutants Gly263→Ala (▼), Arg264→Ala (▲), Leu332→Ala (○), and Leu332→Pro (□). ATPase activity was measured at 37 °C in the presence of 130 mM NaCl, 20 mM KCl, 3 mM ATP, and the indicated vanadate concentrations as specified in Materials and Methods. Average values of data points from three to eight independent measurements are shown as percentage of the Na^+,K^+-ATPase activity measured in the absence of vanadate. The data were analyzed by fitting the Hill equation for inhibition $V = [(V_{max} - V_\infty) - (V_{max} - V_\infty)[L]^n/(K_{0.5}^n + [L]^n)] + V_\infty$, with Hill number $n = 1$ and $V_{max} = 100\%$. V_∞ is the activity of the maximally inhibited enzyme. The extracted $K_{0.5}$ values for vanadate inhibition are shown in Table 3. For all data points, SEM was less than 3%.

the smaller cytoplasmic domain ("domain A" or "β-strand domain") with a long loop extending to transmembrane segment M3 (*9*). Comparison of the two conformations of the Ca^{2+}-ATPase in the E_1Ca_2 and E_2-vanadate crystals suggests that both domain A and M3 move in connection with the conformational change, bringing domain A closer to the catalytic site in the P-domain (*9*). The glycine, which introduces flexibility of the peptide backbone and is required for formation of the hydrogen bonded turn, may be critical to this movement and, thus, to the long-range communication between domain A and the catalytic site.

Titration of ligand dependencies of Na^+,K^+-ATPase activity in the Gly263→Ala and Arg264→Ala mutants showed changes in the apparent affinities relative to wild-type that could be accounted for by a displacement of the E_1-E_2 conformational equilibrium of the dephosphoenzyme in favor of E_1 (Tables 1 and 3). It is particularly noteworthy that the $K_{0.5}$ for ATP was reduced about 8-fold and the $K_{0.5}$ for vanadate increased about 7-fold in Gly263→Ala. Furthermore, the level of the K^+-occluded $E_2(K_2)$ intermediate was reduced in the Gly263→Ala and Arg264→Ala mutants relative to wild-type, the apparent affinity of the K^+-occlusion sites being approximately 80-fold lower in the Gly263→Ala mutant as compared with the wild-type (Figure 8 and Table 3). Since the rate constant characterizing deocclusion of K^+ or Rb^+ was increased as much as 20-fold in the Gly263→Ala mutant relative to the wild-type, the instability of the occluded intermediate seems to be caused mainly by an increased rate of deocclusion.

The steady-state level of the K^+-insensitive and ADP-sensitive E_1P phosphoenzyme was high in the Gly263→Ala and Arg264→Ala mutants under conditions where the K^+-sensitive and ADP-insensitive E_2P phosphoenzyme accumulated in the wild-type (Table 2), compatible with a

displacement of the E_1P-E_2P equilibrium of the phosphoenzyme in favor of E_1P in the mutants. In dephosphorylation experiments carried out starting from the E_1P form, it was moreover demonstrated that the phosphoenzyme of the mutants decayed slowly relative to wild-type, indicative of a reduction of the E_1P to E_2P conversion rate in the mutants. This finding was independent of whether the experiments were carried out at 0 °C or at the more physiological temperature of 25 °C using a quenched-flow technique, and it was also confirmed at a high salt concentration of 600 mM (Figure 5B). The rate coefficient associated with the E_1P to E_2P transition at 25 °C and 200 mM NaCl was reduced as much as 4-fold in the Gly263→Ala mutant and 2-fold in the Arg264→Ala mutant, relative to the wild-type (Table 3).

A central question in our understanding of energy transduction in the Na^+,K^+-ATPase is to what extent the E_1P-E_2P conformational transition of the phosphoenzyme resembles the E_1-E_2 transition of the dephosphoenzyme. On the basis of the results summarized above it may be concluded that for both mutants the E_1P-E_2P equilibrium of the phosphoenzyme and the E_1-E_2 equilibrium of the dephosphoenzyme are displaced in parallel in favor of the E_1 and E_1P forms. This shows that at least in the vicinity of Gly263 similar structural changes may occur in relation to the E_1P-E_2P and E_1-E_2 transitions.

All the observed effects on the conformational equilibria were more pronounced in the Gly263→Ala mutant than in the Arg264→Ala mutant. This difference seems to be reflected also in the maximum turnover number for ATP hydrolysis. In the Gly263→Ala mutant, the maximum turnover number was considerably reduced relative to wild-type, whereas in the Arg264→Ala mutant it was wild-type like or tended to be slightly increased (Table 1). It is possible to account for the difference between the turnover rates of the two mutants on the basis of the observed effects on the partial reaction steps of the cycle. The rate constants for phosphorylation [E_1Na_3 to $E_1P(Na_3)$] and the subsequent interconversion of the phosphoenzyme to E_2P were found to be 138 and 112 s^{-1}, respectively, for the wild-type enzyme at 25 °C. In the presence of K^+, the dephosphorylation of E_2P is known to have a rate constant not less than 300 s^{-1}, and the step limiting the maximum turnover rate of the wild-type is likely to be the K^+ deocclusion, $E_2(K_2)$→E_1, whose rate constant can be estimated to be approximately 70 s^{-1} under comparable conditions at 25 °C and saturating substrate concentrations (*31*, *33*−*35*). Using these rate constants and neglecting the reverse reactions, which must be relatively slow at the prevailing ligand concentrations (*33*), we find by computation according to the model in Scheme 1 that the rate of the E_1P to E_2P transition must be reduced more than 2-fold in order to obtain a substantial reduction in the turnover rate for ATP hydrolysis. The simulation shows that a 4-fold reduction in the rate of the E_1P to E_2P transition, corresponding to the Gly263→Ala mutant, decreases the turnover rate for ATP hydrolysis to approximately half. Under these conditions, the E_1P to E_2P transition has become rate limiting and any increase in the rate of the K^+ deoccluding $E_2(K_2)$ to E_1 transition would be without much influence on the overall rate of ATP hydrolysis. Therefore, the simulation supports the hypothesis that the reduced rate of the E_1P to E_2P transition constitutes the major reason for the reduced turnover rate of the Gly263→Ala mutant. The effect of the Arg264→Ala mutation on the E_1P to E_2P transition is less strong and would be completely masked if the rate of the K^+ deoccluding $E_2(K_2)$ to E_1 step were increased to an extent similar to that seen at nonsaturating ATP concentrations in Figure 8. Thus, the computer simulation shows that the combination of the 2-fold reduction of the rate of the E_1P to E_2P transition seen for the Arg264→Ala mutant with a 4-fold increase in the rate of the $E_2(K_2)$ to E_1 step results in a turnover rate for ATP hydrolysis of 105% relative to wild-type, in line with the wild-type like or slightly increased rate shown in Table 1.

It was previously demonstrated that the mutants Leu332→Pro and Leu332→Ala like the Gly263→Ala and Arg264→Ala mutants are characterized by accumulation of the E_1P form of the phosphoenzyme during turnover (*11*). Leu332 is located at a distance of at least 20 Å from Gly263, at the boundary between the large cytoplasmic domain and transmembrane segment M4 close to the unwound part of the M4 helix thought to be involved in cation binding (*9*, *19*, *28*). In the present study, the mutants Leu332→Pro and Leu332→Ala were further characterized and we found that the rate coefficient associated with the E_1P to E_2P transition at 25 °C was reduced to the same extent (4-fold) in the Leu332→Pro mutant as in the Gly263→Ala mutant, and 2.6-fold in the Leu332→Ala mutant, relative to the wild-type (Table 3). Hence, Leu332, like Gly263, plays an important role in the E_1P to E_2P transition of the phosphoenzyme. It was therefore interesting to elucidate the effects of the Leu332→Pro and Leu332→Ala mutations on the behavior of the dephosphoenzyme, as well, to obtain more information on whether there is an obligatory link between a displacement of the equilibrium between the E_1P and E_2P forms of the phosphoenzyme and a displacement of the equilibrium between the E_1 and E_2 forms of the dephosphoenzyme. The very low vanadate sensitivity and the reduced level of the K^+-occluded $E_2(K_2)$ intermediate in the Leu332→Pro and Leu332→Ala mutants show that indeed the E_1-E_2 conformational equilibrium of the dephosphoenzyme is displaced in favor of the E_1 form in these mutants, and as seen in Table 3, there seems to be a rather good correlation between this displacement and the accumulation of the E_1P phosphoenzyme intermediate. When all the various parameters in Tables 2 and 3 as well as the apparent affinities for ATP, Na^+, and K^+ determined in the ATPase assay (Table 1 and ref *11*) are taken into consideration, Leu332→Pro seems to be the mutant exhibiting the most pronounced displacement of the conformational equilibria in favor of E_1 and E_1P. However, in contrast to the 20-fold acceleration of deocclusion induced by the Gly263→Ala mutation, the mutants Leu332→Pro and Leu332→Ala displayed a wild-type like rate of K^+ deocclusion and only a 3−4-fold increase in the rate of Rb^+ deocclusion (Table 3), suggesting a fundamental difference between Gly263→Ala and the Leu332 mutants: In the Gly263 mutant, the effect of the mutation on the E_1-E_2 conformational equilibrium is caused mainly by an acceleration of the E_2 to E_1 transition, similar to that normally occurring as a result of ATP binding with low affinity (*3*, *4*), but in the Leu332 mutants the displacement of the E_1-E_2 conformational equilibrium must instead be the result of a reduced rate of the reverse E_1 to E_2 transition.

The present observations are of general importance for understanding the mechanism of P-type transport ATPases. In the sarcoplasmic reticulum Ca^{2+}-ATPase, the functional consequences of mutation to the glycine (Gly233) corresponding to Gly263 of the Na^+,K^+-ATPase were strikingly similar to those described here for the Na^+,K^+-ATPase (*21*). Although the effect of the mutation on the E_2 to E_1 transition in the Ca^{2+}-ATPase was less pronounced (2−3-fold acceleration) compared with the 20-fold acceleration observed for the Na^+,K^+-ATPase mutant, it was similar in nature, and the quantitative difference may be explained by the characteristics of the cation being released in this step (H^+ versus K^+). It is furthermore of interest that mutation of the proline (Pro312) at the position in the Ca^{2+}-ATPase corresponding to Leu332 in the Na^+,K^+-ATPase led to a 12-fold decrease in the rate of Ca^{2+} dissociation from the dephosphoenzyme (*21*) equivalent to the decreased E_1 to E_2 transition rate deduced from the present results. The fact that the specific roles of these residues in the energy transducing conformational changes are universal among P-type ATPases strongly supports the view that these enzymes function by a common mechanism.

ACKNOWLEDGMENT

We would like to thank Dr. Jens Peter Andersen for discussion and many helpful suggestions, Jytte Jørgensen, Janne Petersen, Kirsten Lykke Pedersen, and Karin Kracht for expert technical assistance, and Dr. R. J. Kaufman, Genetics Institute, Boston, MA, for the expression vector pMT2.

REFERENCES

1. Albers, R. W. (1967) *Annu. Rev. Biochem. 36*, 727−756.
2. Post, R. L., Kume, S., Tobin, T., Orcutt, B., and Sen, A. K. (1969) *J. Gen. Physiol. 54*, 306s−326s.
3. Post, R. L., Hegyvary, C., and Kume, S. (1972) *J. Biol. Chem. 247*, 6530−6540.
4. Glynn, I. M. (1985) in *The Enzymes of Biological Membranes* (Martonosi, A. N., Ed.) Vol. 3, pp 35−114, Plenum Publishing Corp., New York.
5. Jørgensen, P. L., and Andersen, J. P. (1985) *J. Membr. Biol. 103*, 95−120.
6. Robinson, J. D., and Pratap, P. R. (1993) *Biochim. Biophys. Acta 1154*, 83−104.
7. Karlish, S. J. D. (1980) *J. Bioenerg. Biomembr. 12*, 111−136.
8. Kane, D. J., Fendler, K., Grell, E., Bamberg, E., Taniguchi, K., Froehlich, J. P., and Clarke, R. J. (1997) *Biochemistry 36*, 13406−13420.
9. Toyoshima, C., Nakasako, M., Nomura, H., and Ogawa, H. (2000) *Nature 405*, 647−655.
10. Jørgensen, P. L., and Petersen, J. (1985) *Biochim. Biophys. Acta 821*, 319−333.
11. Vilsen, B. (1997) *Biochemistry 36*, 13312−13324.
12. Boxenbaum, N., Daly, S. E., Javaid, Z. Z., Lane, L. K., and Blostein, R. (1998) *J. Biol. Chem. 273*, 23086−23092.
13. Kunkel, T. A. (1985) *Proc. Natl. Acad. Sci. U.S.A. 85*, 3314−3318.
14. Vilsen, B., Andersen, J. P., Clarke, D. M., and MacLennan, D. H. (1989) *J. Biol. Chem. 264*, 21024−21030.
15. Vilsen, B. (1992) *FEBS Lett. 314*, 301−307.
16. Vilsen, B. (1993) *Biochemistry 32*, 13340−13349.
17. Vilsen, B. (1995) *Biochemistry 34*, 1455−1463.
18. Bradford, M. M. (1976) *Anal. Biochem. 72*, 248−254.
19. Vilsen, B., and Andersen, J. P. (1998) *Biochemistry 37*, 10961−10971.
20. Vilsen, B. (1999) *Biochemistry 35*, 11389−11400.
21. Sørensen, T. L., Dupont, Y., Vilsen, B., and Andersen, J. P. (2000) *J. Biol. Chem. 275*, 5400−5408.
22. Gutfreund, H. (1995) *Kinetics for the Life Sciences*, Cambridge University Press, Cambridge.
23. Inesi, G., Kurzmack, M., and Lewis, D. (1988) *Methods Enzymol. 157*, 154−190.
24. Reynolds, J. A., Johnson, E. A., and Tanford, C. (1985) *Proc. Natl. Acad. Sci. U.S.A.* 82, 3658−3661.
25. Vilsen, B., Ramlov, D., and Andersen, J. P. (1997) *Ann. N. Y. Acad. Sci. 834*, 297−309.
26. Klodos, I., Post, R. L., and Forbush, B., III (1994) *J. Biol. Chem. 269*, 1734−1743.
27. Post. R. L., and Klodos, I. (1996) *Am. J. Physiol. 271*, C1415−C1423.
28. Jewell-Motz, E. A., and Lingrel, J. B. (1993) *Biochemistry 32*, 13523−13530.
29. Mårdh, S. (1975) *Biochim. Biophys. Acta 391*, 448−463.
30. Cornelius, F. (1999) *Biophys. J. 77*, 934−942.
31. Forbush, B., III (1987) *J. Biol. Chem. 262*, 11104−11115.
32. Cantley, L. C., Jr., Cantley, L. G., and Josephson, L. (1978) *J. Biol. Chem. 253*, 7361−7368.
33. Läuger, P. (1991) *Electrogenic Ion Pumps*, Sinauer Assoc., Inc., Sunderland, MA.
34. Glynn, I. M., and Karlish, S. J. D. (1990) *Annu. Rev. Biochem. 59*, 171−205.
35. Kane, D. J., Grell, E., Bamberg, E., and Clarke, R. J. (1998) *Biochemistry 37*, 4581−4591.

BI002367M